

## Article

# Delay Minimization Using Hybrid RSMA-TDMA for Mobile Edge Computing

Fengcheng Xiao, Pengxu Chen, Hua Wu, Yuming Mao and Hongwu Liu \*

<sup>1</sup> School of Information Science and Electrical Engineering, Shandong Jiaotong University, Jinan 250357, China; 21208017@stu.sdjtu.edu.cn (F.X.); cpx17863275219@163.com (P.C.); wuhua@sdjtu.edu.cn (H.W.); 18660106266@163.com (Y.M.)

\* Correspondence: liuhongwu@sdjtu.edu.cn

**Abstract:** Rate-splitting multiple access (RSMA) has recently received attention due to its benefits in both spectral and energy efficiencies. In this paper, we propose a hybrid RSMA-time-division multiple access (TDMA) scheme for a mobile edge computing (MEC) system, where two edge users need to offload their task data to a MEC server. In the proposed scheme, the offloading time is divided into two time phases. Specifically, we design a cognitive radio (CR)-inspired RSMA scheme, in which two users, namely the primary user and secondary user, offload their task data to the MEC server in the first time phase, while only a single user can offload task data in the second time phase. With the aim of minimizing the overall offloading delay, we formulate the offloading delay minimization problem subject to the transmit power and total energy constraints. We transform the original fractional programming non-convex problem to a convex one by using the Dinkelbach transform and propose Dinkelbach and Newton iterative algorithms to determine the optimal transmit power allocation. Specifically, we establish the optimization criteria for the three offloading schemes and derive the corresponding closed-form expressions for the optimal power allocation. Compared to the existing offloading schemes, the numerical results show that the proposed hybrid RSMA-TDMA scheme in scenarios where having a limited energy budget is superior in offloading delay compared to other offloading schemes and the sum offloading delay tends to a constant with the increase in the energy budget.

**Keywords:** mobile edge computing; rate-splitting multiple access; time-division multiple access; offloading delay



**Citation:** Xiao, F.; Wu, H.; Chen, P.; Mao, Y.; Liu, H. Delay Minimization Using Hybrid RSMA-TDMA for Mobile Edge Computing. *Electronics* **2023**, *12*, 2550. <https://doi.org/10.3390/electronics12112550>

Academic Editor: Antonio Brogi

Received: 28 April 2023

Revised: 31 May 2023

Accepted: 2 June 2023

Published: 5 June 2023



**Copyright:** © 2023 by the authors. Licensee MDPI, Basel, Switzerland. This article is an open access article distributed under the terms and conditions of the Creative Commons Attribution (CC BY) license (<https://creativecommons.org/licenses/by/4.0/>).

## 1. Introduction

With the rapid growth of the Internet of Things (IoT) and the increasing number of connected devices in wireless communication systems, various services and applications that utilize wireless communication systems have emerged, terminal users can offload computation-intensive and latency-sensitive tasks to mobile edge computing (MEC) servers [1]. The large amount of computing resources on the MEC servers can be used to help edge users interrupt fast data processing. The authors of [2] investigated a MEC-assisted vehicular network and solved the minimum vehicle computation and system computation problems based on game theory. In [3], the authors surveyed the state of the art of the fixed and mobile edge computing nodes (ECNs) and studied the integrated architectures based on different classifications of ECNs. In [4], the authors studied an unmanned aerial vehicle (UAV)-assisted IoT system and proposed three algorithms to minimize the energy consumption of the terminal nodes and UAV. Traditional time-division multiple access (TDMA) schemes allocate time slots based on the user's offload delay requirements, according to the channel conditions, the authors of [5] investigated a novel TDMA-MEC system to improve energy efficiency.

Massive edge users offload data to MEC servers, which causes a large amount of spectrum to be occupied and results in spectrum scarcity. The emergence of non-orthogonal

multiple access (NOMA) technology has solved the problem of spectrum resource shortage, it is able to allow multiple edge users to transmit simultaneously in blocks of resources of the same frequency [6]. MEC servers can adopt NOMA scheme to improve the offloading performance [7], in [8], for an intelligent reflecting surface (IRS)-aided MEC system, the resource allocation and the IRS beamforming design were jointly optimized to maximize the offloading sum-rate by using alternating optimization (AO) algorithm. Furthermore, the hybrid NOMA scheme has also become a novel scheme for NOMA-assisted MEC (NOMA-MEC) systems [9–13]. The authors in [9] studied a hybrid transmission scheme that combines NOMA and orthogonal multiple access (OMA) for MEC systems, in which a lower priority user first offloaded its tasks together with a higher priority user by NOMA transmission and then offloaded the remaining tasks using OMA transmission, or until the high priority user finished offloading, the power allocation of the lower priority user was optimized to minimize offloading delay subject to its energy budget. Furthermore, the works in [10] aimed to optimize the power allocation of two users subject to their respective power and energy budgets for the NOMA-MEC system. They designed an efficient algorithm to solve it based on the successive convex approximation (SCA) method. Furthermore, based on a multi-user NOMA-MEC system, a two-user NOMA iterative scheme was devised in [11] to reduce offloading delay, the single user power allocation was optimized to minimize the offloading delay subject to the maximum power constraint and the maximum energy constraint, respectively. The authors in [12] studied an IRS-aided MEC system and proposed a flexible time-sharing NOMA scheme to minimize offloading delay and computing delay. The results of [13] showed that compared with OMA and NOMA, the hybrid NOMA scheme could achieve lower energy consumption. Note that TDMA is used for OMA in this paper.

More recently, rate-splitting multiple access (RSMA) has become a promising technology to enhance the spectrum and energy efficiency, low latency, and high reliability of both downlink and uplink communication systems [14–16]. In uplink RSMA, all the split streams are fully decoded at the base station (BS) [17]. Unlike uplink RSMA, in the downlink, RSMA operates by splitting messages into common and private streams, with common streams being jointly encoded and decoded by all users. In contrast, private streams are individually encoded and decoded by each user. After decoding and subtracting the common stream by successive interference cancellation (SIC), each user decodes their desired private stream by regarding other private streams as interference [18–20]. Several recent studies have shown that RSMA plays an important role in achieving high energy and spectral efficiency in unmanned aerial vehicle (UAV) networks [21]. A rate-splitting NOMA scheme was proposed in [22] to reduce the complicated user pairing schemes. In [23], the authors proposed two RS strategies, namely fixed RS and cognitive RS, to enhance user fairness and improve outage performance. In [24], the sum-rate problem for the uplink RSMA system was investigated and the optimal decoding order was obtained by using an exhaustive search method. With the benefits of MEC and RSMA, MEC and RSMA were used for aerial networks aiming to enhance computation and communication [25]. In [26], the authors proposed a rate splitting (RS) strategy for the uplink CR-inspired NOMA system. They analyzed the outage performance for the secondary user (SU) without deteriorating the primary user (PU)'s outage performance. With the benefits of MEC, the authors of [27] utilized a CR-inspired RSMA scheme to allow SU to offload tasks to the MEC server with a dynamic rate splitting factor while ensuring no interference to the offloading performance of PU. In [28], the authors investigated the impact of user locations on the performance of a MEC system using RSMA. They derived a closed-form expression for the successful computation probability in the presence of randomly deployed users, which enabled them to analyze the effects of user locations on offloading performance. Table 1 provides the main studies and methods of the current references, and compares our proposed scheme with them.

**Table 1.** Comparison with other schemes of references.

	[7]	[9]	[10]	[12]	[25]	[28]	Proposed Scheme
NOMA scheme	✓	✓	✓	✓			
RSMA scheme					✓	✓	✓
Hybrid transmission scheme		✓	✓	✓			✓
Optimal power allocation	✓	✓	✓	✓			✓
Energy budget		✓	✓				✓
Offloading delay minimization	✓	✓	✓	✓			✓

To the best of our knowledge, there is a lack of research on offload delay minimization for RSMA schemes. To further investigate the effect of the hybrid offloading scheme on MEC, in this paper, we propose a hybrid RSMA-TDMA scheme to minimize offloading delay for a MEC system to further reduce offloading delay. Specifically, in the proposed scheme, we divide the offloading phase into two phases. In the first phase, we design a CR-inspired RSMA strategy. Depending on the energy available at the user, three cases are identified, we formulate a minimum offloading delay problem, and the power allocation of SU for two offloading phases is optimized subject to energy and power constraints. In the second phase, the proposed scheme allows only a single user to offload tasks to the MEC server. The detailed contributions of our work are summarized as follows.

- We propose a hybrid RSMA-TDMA scheme to assist MEC with task offloading. In the proposed scheme, the offloading phase is divided into two phases. In the first phase, two edge users utilize the CR-inspired RSMA scheme to offload their computation tasks to a MEC server, while the second phase is allocated to a single user for task offloading. Specifically, If one user also has remaining computation tasks, the user will occupy an independent time phase for task offloading.
- We formulate an offloading delay minimization problem for a hybrid RSMA-TDMA scheme. Subject to the user's different energy budget, three offloading scenarios are considered, i.e., TDMA, hybrid RSMA-TDMA, and RSMA. In the hybrid RSMA-TDMA, we develop an iterative algorithm by approximating the original problem into a convex one with Dinkelbachs' method. The power allocation expressions of two phases are derived by Karush–Kuhn–Tucker (KKT) conditions.
- Numerous results reveal the superiority of the proposed hybrid RSMA-TDMA scheme compared with other schemes. Particularly, in the proposed scheme, with the increased target rate of PU, the chosen hybrid RSMA-TDMA scheme will become a hybrid NOMA-TDMA scheme.

## 2. System Model and CR-inspired RSMA Scheme

### 2.1. System Model

In this paper, we consider an uplink RSMA-MEC system, which consists of two edge users, namely  $U_a$  and  $U_b$ , a MEC server, two edge users need to offload all their computing tasks to a MEC server. In the proposed scheme, we assume that each user is equipped with a single antenna, and the number of bits contained in  $U_k$ 's tasks as  $N_k$ , where  $k \in \{a, b\}$ . Similarly to [6,9,11,29], we also assume that the task computing delay from the MEC server is not considered, this is because the MEC servers have sufficient computing resources compared with offloading delay, and the task computing delay is negligible. The task computing delay (e.g., references [7,30]) will be studied in future work.

In the considered system, as shown in Figure 1, we assume that  $U_a$  has a higher priority than  $U_b$ ,  $U_a$  offloads its task data over the entire bandwidth, while  $U_b$  can either offload its task data simultaneously with  $U_a$  or wait until  $U_a$  finishes offloading. Specifically, in the first time phase  $t_1$ ,  $U_b$  offloads its task data together with  $U_a$  by using the RSMA

scheme, and  $U_a$ 's task data is completely offloaded. The data signal transmitted by  $U_a$  as  $x_a$ , while the data signal transmitted by  $U_b$  as  $x_{b,1}$ . In the second phase  $t_2$ ,  $U_b$  offloads the remaining task data, the data signal is denoted as  $x_{b,2}$ . Specifically, in the first phase  $t_1$ ,  $U_b$  splits its signal  $x_{b,1}$  into two streams  $x_{b,11}$  and  $x_{b,12}$  by using the determined rate splitting parameters.

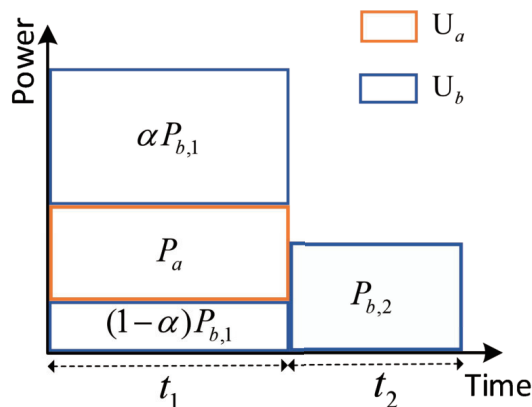


Figure 1. Proposed hybrid RSMA-TDMA scheme for MEC system.

By applying the proposed hybrid RSMA-TDMA scheme, the received signal at the MEC server during the first time phase  $t_1$  can be expressed as

$$y_1 = \sqrt{P_a \ell_a} h_a x_a + \sqrt{\alpha P_{b,1} \ell_b} h_b x_{b,11} + \sqrt{(1-\alpha) P_{b,1} \ell_b} h_b x_{b,12} + n, \tag{1}$$

where  $P_a$  is the transmission power of  $U_a$ ,  $h_k$  is the channel gain,  $\ell_k \triangleq (\frac{d_k}{d_0})^{-\chi}$  denotes the path-loss with the distance from  $U_k$  to the MEC server,  $d_k$  is the distance between the MEC server and  $U_k$ ,  $d_0$  denotes the reference distance,  $\chi$  is the path loss exponent,  $n$  is the white Gaussian noise with zero mean and variance  $\sigma^2$ , and  $\alpha$  is power allocation factor satisfying  $0 \leq \alpha \leq 1$ .

Then, the received signal at the MEC server in the second phase  $t_2$  can be expressed as

$$y_2 = \sqrt{P_{b,2} \ell_b} h_b x_{b,2} + n, \tag{2}$$

where  $P_{b,1}$  and  $P_{b,2}$  are the  $U_b$ 's transmission power in two time phases, respectively.

During the first time phase  $t_1$ , the decoding order at the MEC server is  $x_{b,11} \rightarrow x_a \rightarrow x_{b,12}$ , which is designed to maximize the achievable rate of  $U_b$  [26]. The signal-to-noise-ratio (SNR) for decoding  $x_{b,11}$ ,  $x_a$ ,  $x_{b,12}$  at the MEC server can be expressed as

$$\gamma_{b,11} = \frac{\alpha \rho_{b,1} |h_b|^2}{\rho_a |h_a|^2 + (1-\alpha) \rho_{b,1} |h_b|^2 + 1}, \tag{3}$$

$$\gamma_a = \frac{\rho_a |h_a|^2}{(1-\alpha) \rho_{b,1} |h_b|^2 + 1}, \tag{4}$$

and

$$\gamma_{b,12} = (1-\alpha) \rho_{b,1} |h_b|^2, \tag{5}$$

respectively, where  $\rho_a \triangleq \frac{P_a \ell_a}{\sigma^2}$ , and  $\rho_{b,1} \triangleq \frac{P_{b,1} \ell_a}{\sigma^2}$ .

In the remaining time phase  $t_2$ , the SNR at the MEC server for decoding  $x_{b,2}$  can be expressed as  $\gamma_{b,2} = \rho_{b,2} |h_b|^2$ , where  $\rho_{b,2} \triangleq \frac{P_{b,2} \ell_a}{\sigma^2}$ .

Assuming that  $B$  is the allocated bandwidth for  $U_a$  and  $U_b$ , the achievable rates for transmitting  $x_a$ ,  $x_{b,1}$ , and  $x_{b,2}$  can be, respectively, expressed as  $R_a = B \log_2(1 + \gamma_a)$ ,  $R_{b,1} = R_{b,11} + R_{b,12}$ , and  $R_{b,2} = B \log_2(1 + \gamma_{b,2})$ , in which  $R_{b,11} = B \log_2(1 + \gamma_{b,11})$  and  $R_{b,12} = B \log_2(1 + \gamma_{b,12})$ .

### 2.2. CR-Inspired RSMA Scheme

Inspired by the CR principles, the  $U_a$  and  $U_b$  are treated as PU and SU, respectively, then we design a CR-inspired RSMA scheme, the SU offloads its task data to the MEC server when the offloading performance of PU can be guaranteed to be the same as that of the OMA. In the first phase, the CR-inspired RSMA scheme aims to maximize the achievable rate of the  $U_b$  without causing interference to the  $U_a$ 's offloading performance, i.e., the outage probability of  $U_a$  is the same as OMA. This is achieved by utilizing a decoding order of  $x_{b,11} \rightarrow x_a \rightarrow x_{b,12}$  for successive interference cancellation (SIC) processing at the MEC server. To ensure that  $x_a$  and  $x_{b,12}$  do not impact the offloading performance of  $U_a$  during SIC processing, the MEC server sends an interference threshold  $\tau = \max \left\{ 0, \frac{\rho_a |h_a|^2}{\varepsilon_a} - 1 \right\}$  to  $U_b$ , where  $\varepsilon_a \triangleq 2^{\frac{\hat{R}_a}{B}} - 1$  with  $\hat{R}_a$  representing the target rate of  $U_a$ .

The rate splitting and power allocation parameters are designed based on  $U_b$ 's channel state information (CSI) and  $\tau$ , and the optimal parameters are determined for the following cases:

(1)  $0 < \rho_{b,1} |h_b|^2 \leq \tau$ . The task bits can be successfully offloaded to the MEC server when  $\tau > 0$ , which means that the condition  $\log_2(1 + \gamma_a) \geq \hat{R}_a$  is satisfied. In order to maximize  $R_{b,1}$ ,  $\alpha$  should be set as  $\alpha = 0$ , and rate splitting factor  $\beta$  should be set as  $\beta = 0$ . The decoding order at MEC server is  $x_a \rightarrow x_{b,12} = x_{b,1}$ , the achievable rate of  $U_a$  is

$$R_a^{(I)} = \log_2 \left( 1 + \frac{\rho_a |h_a|^2}{\rho_{b,1} |h_b|^2 + 1} \right) \tag{6}$$

and the achievable rate of  $U_b$  is

$$R_{b,1}^{(I)} = R_{b,12}^{(I)} = \log_2 (1 + \rho_{b,1} |h_b|^2). \tag{7}$$

(2)  $0 < \tau < \rho_{b,1} |h_b|^2$ . To maximize  $R_{b,1}$ , rate-splitting should be conducted at  $U_b$ , the parameter  $\alpha$  should be chosen to satisfy  $\log_2 (1 + (1 - \alpha)\rho_{b,1} |h_b|^2) = \log_2(1 + \tau)$ , which leads to  $\alpha = 1 - \frac{\tau}{\rho_{b,1} |h_b|^2}$ . Therefore, the achievable rate of  $U_a$  can be expressed as

$$R_a^{(II)} = \log_2 \left( 1 + \frac{\rho_a |h_a|^2}{\tau + 1} \right) \tag{8}$$

and the achievable rate of  $U_b$  is

$$R_{b,1}^{(II)} = R_{b,11}^{(II)} + R_{b,12}^{(II)} = \log_2 \left( 1 + \frac{\rho_{b,1} |h_b|^2 - \tau}{\rho_a |h_a|^2 + \tau + 1} \right) + \log_2(1 + \tau). \tag{9}$$

In the proposed RSMA scheme, the target rate can be expressed as  $\hat{R}_{b,12} = \log_2(1 + \tau)$ . Since we have  $\hat{R}_{b,12} = (1 - \beta)\hat{R}_{b,1}$ , we can obtain the optimal rate splitting factor as  $\beta^* = 1 - \frac{B(\log_2(\rho_a |h_a|^2) - \log_2(\varepsilon_a))}{\hat{R}_{b,1}}$ , where  $\hat{R}_{b,1} = \frac{\bar{N}_b}{t_1}$  with  $\bar{N}_b$  denoting that the offloading task bits of the first time phase  $t_1$ .

(3)  $\tau = 0$ . In this case, since the task bits cannot be offloaded successfully, the transmitting power should be fully allocated to transmit  $x_{b,1}$ , which means  $\alpha = 1$  and  $\beta = 1$ . The decoding order at the MEC server is  $x_{b,1} = x_{b,11} \rightarrow x_{b,12}$ , the achievable rate of  $U_a$  is

$$R_a^{(III)} = \log_2(1 + \rho_a |h_a|^2), \tag{10}$$

and the achievable rate of  $U_b$  can be denoted as

$$R_{b,1}^{(III)} = R_{b,11}^{(III)} = \log_2\left(1 + \frac{\rho_{b,1} |h_b|^2}{\rho_a |h_a|^2 + 1}\right). \tag{11}$$

In the second phase of using the TDMA scheme, the achievable rate of  $U_b$  can be expressed as

$$R_{b,2} = \log_2(1 + \rho_{b,2} |h_b|^2). \tag{12}$$

### 3. Offloading Delay Minimization

In this paper, we focus on offloading delay minimization of the proposed hybrid RSMA-TDMA scheme-assisted MEC system. With the assumption that  $U_b$  offloads its task data using RSMA transmission along with  $U_a$ , and if there is any remaining task data after the RSMA transmission,  $U_b$  continues offloading using TDMA transmission. Thus, an optimization problem is formulated to minimize the offloading delay of two users. The offloading delay minimization problem can be formulated as

$$(P1) : \min_{P_{b,1}, P_{b,2}} t_1 + t_2 \tag{13}$$

$$\text{s.t. } t_2 \geq 0, \tag{13a}$$

$$t_1 P_{b,1} + t_2 P_{b,2} \leq E, \tag{13b}$$

$$P_{b,1} \geq 0, \tag{13c}$$

$$P_{b,2} \geq 0, \tag{13d}$$

where  $t_2 \triangleq \frac{N_b - t_1 R_{b,1}}{R_{b,2}}$ . Constraint (13a) represents user  $U_b$  not finishing its offloading before user  $U_a$ . Constraint (13b) represents the energy constraint of the user  $U_b$  and  $E$  denotes the total energy constraint of  $U_b$ . Constraints (13c) and (13d) denote the transmission power of the user  $U_b$  in two time phases is non-negative.

Denote  $E_1 = \frac{v \tilde{h}_b^{-1} (N_b - t_1 \log_2(1 + (1 - 2^{-\omega_a})\tau))}{\log_2(1 + v)}$ , and  $E_2 = t_1 2^{\omega_b} \tilde{h}_b^{-1} (2^{\omega_b} - 1 - \tau + 2^{-\omega_a} \tau)$ ,

where  $v = (2^{\omega_a} - 1)(1 + \tau)$ ,  $\omega_k = \frac{N_k}{t_1 B}$ , and  $\tilde{h}_k = \frac{\ell_k |h_k|^2}{\sigma^2}$ .  $E_1$  and  $E_2$  are the energy thresholds that select the TDMA scheme, RSMA scheme, or hybrid RSMA-TDMA scheme. For the task offloading scheme, we need to consider the following scenarios:

**Remark 1.** According to (9), we can obtain the achievable rate of  $U_b$ , i.e.,  $R_{b,1}^{(II)}$ . If  $U_a$  and  $U_b$  offload tasks simultaneously using the RSMA scheme, the minimization energy can be expressed as  $P_{b,1} = \frac{E_2}{t_1}$ , then, by substituting  $P_{b,1}$  into  $t_1 R_{b,1}^{(II)} = N_b$ , it can easily obtain the energy threshold  $E_2$ .

**Remark 2.** By using the inverse method, in case 2 of the following scenarios, we obtain the optimal power allocation expressions of two phases, according to [9], while  $\mu \rightarrow E^{-1} \tilde{h}_b^{-1} (2^{\omega_a} - 1)(1 + \tau)$ , leading to  $P_{b,1}^*(\mu) \rightarrow 0$ ,  $P_{b,2}^*(\mu) \rightarrow \tilde{h}_b^{-1} (2^{\omega_a} - 1)(1 + \tau)$ , then, we can obtain

$$F(\mu) = -\mu (N_b - t_1 \log_2(1 + \tau - 2^{-\omega_a} \tau)) + \log_2(1 + (2^{\omega_a} - 1)(1 + \tau)). \tag{14}$$

Due to the limitation of  $F(\mu) > 0$  when  $\mu \rightarrow E^{-1} \tilde{h}_b^{-1} (2^{\omega_a} - 1)(1 + \tau)$  [9], by applying algebraic operation, we can obtain the energy threshold  $E_1$ .

3.1. Case 1:  $E \leq E_1$

This corresponds to the case where the  $U_b$  has not enough energy to offload the task, and we should consider using TDMA for task offloading, i.e.,  $P_{b,1}^* = 0$ . Since  $P_{b,1}^* = 0$ , all the energy needed to allocate the second phase to minimize offloading delay, the power allocation, and the time allocation expressions can be obtained in a straightforward way, we have

$$N_b = t_2 \log 2 \left( 1 + P_{b,2} \tilde{h}_b^{-1} \right), \tag{15}$$

$$t_2 P_{b,2} \leq E. \tag{16}$$

To minimize offloading delay  $t_2$ , all energy should be used, i.e.,  $t_2 P_{b,2} = E$ , by using the Lambert-W function, we have

$$P_{b,2}^* = \frac{-W \left( -\frac{N_b}{E \tilde{h}_b} 2^{-\frac{N_b}{E \tilde{h}_b}} \ln 2 \right)}{\ln 2 N_b / E} - \tilde{h}_b^{-1}, \tag{17}$$

where  $W(x)$  is the Lambert-W function. In addition,  $t_2^* = \frac{E}{P_{b,2}^*}$ , the sum offloading delay can be expressed as  $T^* = \frac{N_a}{\log_2(1 + \rho_a |h_a|^2)} + t_2^*$ .

3.2. Case 2:  $E_1 < E < E_2$

This corresponds to the case where the user  $U_b$  has not enough energy to use RSMA for task offloading. Since  $t_1$  is known in this letter, i.e.,  $t_1 = \frac{N_a}{R_a}$ , note that  $t_2$  is the ratio of two functions of  $P_{b,1}$  and  $P_{b,2}$ . The objective function in (P1) is fractional and non-convex. Therefore, the Dinkelbach method is leveraged to transform the original problem into an equivalent objective function. By using the fact that  $N_a = t_1 \log_2 \left( 1 + \frac{\rho_a |h_a|^2}{\tau + 1} \right)$ . Since in the hybrid RSMA-TDMA transmission, the time for a single user's offloading is always non-negative, constraint (13a) can be omitted. Then, the principle of Dinkelbach's method is to convert the original format into the following optimization problem as

$$(\mathbf{P2}) : \max_{P_{b,1}, P_{b,2}} F(\mu) \tag{18}$$

$$\text{s.t. } t_1 P_{b,1} + \mu^{-1} P_{b,2} \leq E, \tag{18a}$$

$$P_{b,1} \geq 0, \tag{18b}$$

$$P_{b,2} \geq 0, \tag{18c}$$

where  $F(\mu) \triangleq -\mu(N_b - t_1 \log_2(1 + \tau - 2^{-\omega_a} \tau + 2^{-\omega_a} \rho_{b,1} |h_b|^2)) + \log_2(1 + \rho_{b,2} |h_b|^2)$ ,  $\mu$  is an auxiliary variable that is determined by the proposed iterative algorithm in the later section.

**Lemma 1.** For a given  $\mu$ , the optimal power allocation for problem (P2) is given by

$$P_{b,1}^* = \frac{E - \mu^{-1} \tilde{h}_b^{-1} (2^{\omega_a} - 1)(1 + \tau)}{t_1 + \mu^{-1}}, \tag{19}$$

$$P_{b,2}^* = \frac{E + t_1 \tilde{h}_b^{-1} (2^{\omega_a} - 1)(1 + \tau)}{t_1 + \mu^{-1}}. \tag{20}$$

**Proof.** See Appendix A.  $\square$

To find the optimal value  $\mu$ , two iterative algorithms are proposed to iteratively update the power allocation solutions and the iterative variable. For Dinkelbach's iterative

algorithm, the procedure of this proposed scheme is summarized in Algorithm 1. With the increase in  $l$ , the Dinkelbach iterative variable  $\mu$  will finally converge to the  $\eta$ -optimal  $\mu^*$ , where the  $\eta$ -optimal  $\mu^*$  can be achieved if  $F(\mu^*) \geq \eta$ . The convergence of Dinkelbach’s method-based algorithm was proved in [9,31], and the simulation result also shows that the proposed algorithm is able to converge within a few iterations, which is presented later in the following. Therefore, we also give the Newton iterative algorithm to obtain the optimal power allocation of  $U_b$  as shown in Algorithm 2 of the next page.

---

**Algorithm 1** Power allocation algorithm-based Dinkelbach iterative method

---

**Input:** System bound  $B$ , user information  $P_a, \hat{R}_a, N_a, N_b, \sigma^2$ , channel information  $\ell_a, h_a, \ell_b, h_b$ .

**Output:** Power allocation  $P_{b,1}, P_{b,2}$ , rate splitting factor  $\beta$ , power allocation factor  $\alpha$ , and time phase  $t_2$ .

1: Initialization: Set  $l = 0, \mu_0 = +\infty, \eta = -10^{-10}, P_{b,1}$ , and  $P_{b,2}$ .

2: **repeat**

3:  $l = l + 1$ .

4: Obtain  $P_{b,1}^{(l)}$  and  $P_{b,2}^{(l)}$  based on  $\mu = \mu^{(l-1)}$ .

5: Solve  $F(\mu^{(l)})$  based on  $P_{b,1}^{(l)}$  and  $P_{b,2}^{(l)}$ .

6: Update  $\mu$  as

$$\mu^{(l)} = \frac{\log_2(1 + \rho_{b,2}|h_b|^2)}{N_b - t_1 \log_2(1 + \tau - 2^{-\omega_a} \tau + 2^{-\omega_a} \rho_{b,1}|h_b|^2)}.$$

7: **until**  $F(\mu^{(l)}) \geq \eta$

8:  $P_{b,1}^* = P_{b,1}^{(l)}$ , and  $P_{b,2}^* = P_{b,2}^{(l)}$ .

9:  $\alpha^* = 1 - \frac{\tau}{\rho_{b,1}^*|h_b|^2}$ .

10:  $\beta^* = 1 - \frac{B(\log_2(\rho_a|h_a|^2) - \log_2(\epsilon_a))}{R_{b,1}}$ .

11: **end**

---



---

**Algorithm 2** Power allocation algorithm based Newton iterative method

---

**Input:** System bound  $B$ , user information  $P_a, \hat{R}_a, N_a, N_b, \sigma^2$ , channel information  $\ell_a, h_a, \ell_b, h_b$ .

**Output:** Power allocation  $P_{b,1}, P_{b,2}$ , rate splitting factor  $\beta$ , power allocation factor  $\alpha$ , and time phase  $t_2$ .

1: Initialization: Set  $l = 0, \mu_0 = +\infty, \eta = -10^{-10}, P_{b,1}$ , and  $P_{b,2}$ .

2: **repeat**

3:  $l = l + 1$ .

4: Update  $\mu$  as

$$\mu^{(l+1)} = \mu_l - \frac{F(\mu_l)}{F'(\mu_l)}.$$

5: **until**  $F(\mu^{(l)}) \geq \eta$

6: Obtain  $P_{b,1}^*$ , and  $P_{b,2}^*$ .

7: **end**

---

3.3. Case 3:  $E \geq E_2$

This corresponds to the case where the user  $U_b$  has enough energy to use RSMA for task offloading, and the minimal  $t_2$  can be achieved by using RSMA, i.e.,  $P_{b,2}^* = 0$ . Since  $P_{b,2}^* = 0$ , all the energy is consumed in the first time phase to minimize offloading delay, which means  $P_{b,1}^* = \frac{E}{t_1}$ . The sum offloading delay can be expressed as  $T^* = t_1$ .

**Remark 3.** From about three cases, we can easily obtain that the TDMA scheme has more offloading delay compared to the hybrid RSMA-TDMA scheme when the energy budget of  $U_b$  is higher, the hybrid RSMA-TDMA will become the RSMA scheme when adopting the CR-inspired RSMA

scheme, the sum offloading delay depends on the offloading delay of  $U_a$ ; then, the sum offloading delay tends to a constant. It is due to the design of the CR-inspired RSMA guarantee that the outage probability of  $U_a$  is the same as OMA, the achievable rate of  $U_a$  is the target rate.

For cases 1 and 3, the optimal power allocation expressions of  $U_b$  can be directly obtained, then the complexity can be expressed as  $\mathcal{O}(1)$ . For case 2, due to adopting the Dinkelbach method to transform the original problem to a convex problem, the optimal power allocation expressions of  $U_b$  can be directly obtained by (18) and (19); thus, the complexity is  $\mathcal{O}(I_d)$ , which  $I_d$  is the number of iterations for Dinkelbach's algorithm to converge. For the Newton method-based algorithm, the complexity is  $\mathcal{O}(I_n)$ , where  $I_n$  is the number of iterations for Newton's algorithm to converge.

#### 4. Numerical Results

In this section, we present and discuss the numerical results to evaluate the performance of the proposed hybrid RSMA-TDMA scheme. Unless otherwise specified, the simulation settings are listed as follows:  $\hat{R}_a = 2$  bps/Hz. The normalized channel gains are adopted so as to clearly demonstrate the impact of the channel conditions on the latency [9], we set  $\tilde{h}_i = \frac{\ell_i |h_i|^2}{\sigma^2}$ .

In Figure 2, we present a comparison of the offloading delay achieved by the proposed hybrid RSMA-TDMA scheme with the TDMA scheme and the hybrid NOMA-TDMA scheme proposed in [9] in different energy budgets  $E$ . For both transmission schemes, the offloading delay decreases with the growth of the energy budget, and the offloading delay of TDMA scheme is higher than other schemes. Moreover, the case of higher channel gain has lower latency. When we use the hybrid RSMA-TDMA scheme with same channel gains, the achievable rate of  $U_b$  in the first phase is much larger than the hybrid NOMA-TDMA scheme, and the achievable rates of both users in the remaining time phase have a small gap, although the offloading delay generated in the first stage of the hybrid RSMA-TDMA scheme is higher than the offloading delay generated in the first phase of the hybrid NOMA-TDMA scheme, due to the superiority of the CR-inspired RSMA scheme in the first time phase,  $U_b$  can achieve the maximum possible transmission rate without interfering with the offloading performance of the  $U_a$ , the offloading delay generated in the second time phase will become lower. It can be seen from the plot that, under the setting of  $\tilde{h}_b = 1.5$ , as the energy budget  $E$  increases, the offloading delay of the hybrid RSMA-TDMA scheme remains fixed at 7.5 s. This is due to the fact that the energy budget sufficiently supports both users offloading their task data using the CR-inspired RSMA scheme, i.e., Case 3. Compared to other offloading schemes, it can be seen that the proposed hybrid RSMA-TDMA scheme has superior performance under a limited energy budget. Next, we illustrate the offloading delay obtained with different hybrid schemes and the corresponding power allocation. Compared to other offloading schemes, it can be seen that the proposed hybrid RSMA-TDMA scheme has superior performance under a limited energy budget. We then present the offloading delay when different hybrid schemes are selected, along with the power allocation. The numerical results are shown in Table 2. As shown in Figure 2, the offloading delay decreases with the increasing energy budget, in the proposed scheme, the energy threshold that supports the selection of the RSMA scheme is less than the energy threshold that supports the selection of the NOMA scheme; therefore, with the energy threshold tending to 60 J, the offloading delay tends to 7.5 s.

Figure 3 illustrates the offloading delay curves for the data size. In Figure 3, it can be observed that the offloading delay increases among three offloading schemes as the amount of offloading data size increases, while it decreases as the energy budget increases. This is due to having a sufficient energy budget to enable all tasks to be completed in the first phase. We can also note that with the same energy budget, the NOMA-TDMA scheme converges to the OMA scheme as the amount of offloaded data increases, due to the fact that the increase in the amount of offloaded data leads to the inability to allocate enough energy to utilize the NOMA scheme for task offloading in the first phase. We also note

that the hybrid NOMA-TDMA scheme converges to the OMA scheme as the amount of offloaded data increases at the same energy budget, due to the fact that the increase in the amount of offloaded data leads to the inability to allocate enough energy to utilize the NOMA scheme for task offloading in the first stage. Moreover, the proposed RSMA scheme can take advantage of the low energy budget due to the fact that the threshold value of using hybrid RSMA-TDMA scheme will be lower than that of the hybrid NOMA-TDMA scheme; therefore, a greater benefit can be obtained at low energy budget.

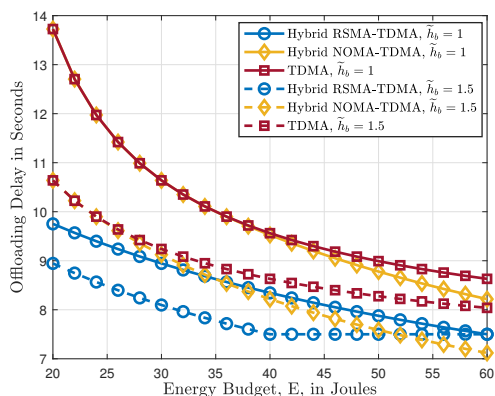


Figure 2. Offloading delay in different energy budget settings.

Table 2. The power allocation of both schemes in different energy budget settings.

(a) Hybrid RSMA-TDMA scheme				
$P_{b,1}$	$P_{b,2}$	$t_2$	Energy Budget	Offloading Delay
4.0851	11.0851	0.8446	40	8.3446
5.0413	12.0413	0.5971	45	8.0971
7.7988	14.7988	0.0344	59	7.5344
(b) Hybrid NOMA-TDMA scheme				
$P_{b,1}$	$P_{b,2}$	$t_2$	Energy Budget	Offloading Delay
0.8739	7.8739	4.5251	40	9.5251
1.7683	8.7683	4.1238	45	9.1238
4.3702	11.3702	3.2672	59	8.2672

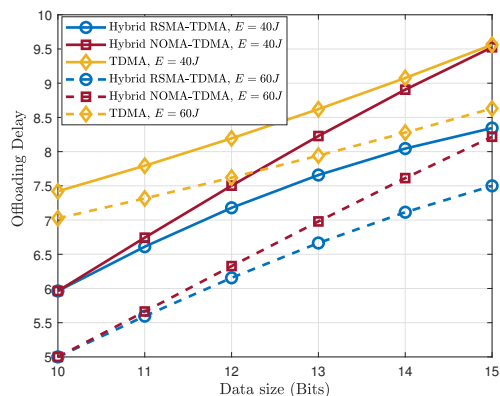


Figure 3. The relationship between data size and offloading delay.

Furthermore, the effect of target rate  $\hat{R}_a$  on the minimum energy threshold and the maximum energy threshold for using the hybrid RSMA-TDMA scheme is shown in Figure 4.  $E_{max}$  and  $E_{min}$  denote the minimum energy threshold and the maximum energy threshold for using hybrid NOMA-TDMA scheme [9], respectively. With the increase in target rate  $\hat{R}_a$ , the energy thresholds  $E_1$  and  $E_2$  tend to  $E_{min}$  and  $E_{max}$ , respectively. It can also be seen that the hybrid RSMA-TDMA scheme tends to the hybrid NOMA-TDMA scheme with the increase in  $\hat{R}_a$ .

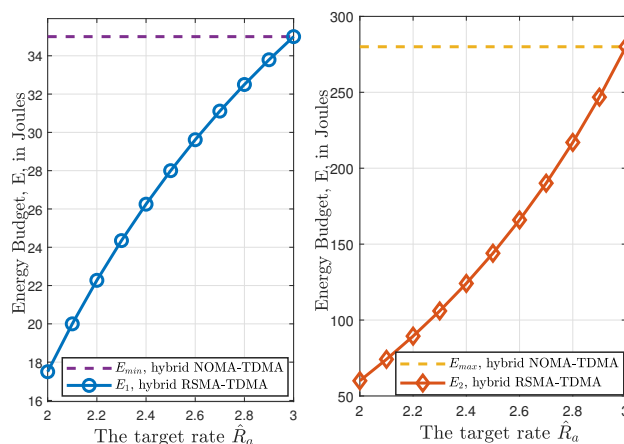


Figure 4. The relationship between energy budget and target rate  $\hat{R}_a$ .

The performance of the proposed algorithm and the effect of different energy budgets and tasks of two users are shown in Figure 5. The increase in energy budget  $E$  leads to the decrease in offloading delay because a higher energy budget leads to an increase in power allocation and decrease in remaining offloading time  $t_2$  according to (18) and (19). The numerical results further confirm that the algorithm can efficiently converge within a few iterations regardless of the parameters. Comparing the two iterative methods, although both methods have the same effect in fractional programming, fewer iterations are required for the Newton iteration method compared to the Dinkelbach iteration method.

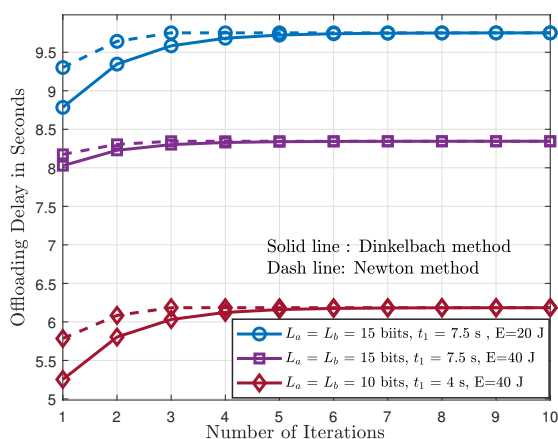


Figure 5. The convergence performance in different parameter settings.

5. Conclusions

In this letter, we proposed a hybrid RSMA-TDMA scheme for a MEC system. The offloading phase was divided into two time phases, and a CR-inspired RSMA scheme was designed in the first time phase. In this phase, we treated two edge users as PU and SU, respectively, SU offloaded its task data together with PU by CR-inspired RSMA scheme,

while the remaining time phase was allocated to a single user to offload the task data. We investigated three different offloading scenarios based on the energy threshold. To minimize offloading delay, we formulated a generic problem for the three offloading scenarios to determine the users’ power allocation. Despite the non-convexity of the formulated problem, we adopted Dinkelbach’s method to transform the original problem into a convex one, two iterative algorithms based on Dinkelbach and Newton’s iterative methods were proposed. The convergence of the proposed algorithm has been proven. Meanwhile, numerical results have verified the performance superiority of the proposed scheme compared with the hybrid NOMA-TDMA scheme and TDMA scheme in the limited region and the sum offloading delay tends to a constant with the increase in energy budget.

**Author Contributions:** Conceptualization, F.X., P.C.; methodology, F.X., P.C. and H.W.; software, F.X., P.C.; validation, F.X., P.C. and Y.M.; formal analysis, F.X., H.W. and Y.M.; investigation, F.X. and P.C.; resources, H.W., Y.M. and H.L.; data curation, F.X.; writing—original draft preparation, F.X., P.C.; writing—review and editing, H.W., Y.M. and H.L.; visualization, H.L.; supervision, H.W. and H.L.; project administration, H.W. and H.L.; funding acquisition, H.W. and H.L.. All authors have read and agreed to the published version of the manuscript.

**Funding:** This work was supported in part by the National Natural Science Foundation of China under Grant 62071202, in part by the Shandong Provincial Natural Science Foundation under Grant ZR2020MF009, and in part by the Research Fundation of Shandong Jiaotong University.

**Institutional Review Board Statement:** Not applicable.

**Informed Consent Statement:** Not applicable.

**Data Availability Statement:** Not applicable.

**Acknowledgments:** The authors gratefully acknowledge all the Reviewers for their positive and valuable comments and suggestions regarding our manuscript.

**Conflicts of Interest:** The authors declare no conflict of interest.

### Appendix A

The proof of the Lemma 1 can be completed by studying the possible choices of  $\lambda_i, \forall i \in \{1, 2, 3\}$ , and showing that the solutions for the case with  $\lambda_i = 0, \forall i \in \{1, 2\}$  yield the smallest offloading delay.

Problem (P2) is convex for a fixed  $\mu$ , we define Lagrangian function as  $L(P_{b,1}, P_{b,2}, \lambda_1, \lambda_2, \lambda_3) \triangleq F(\mu) - \lambda_1 P_{b,1} - \lambda_2 P_{b,2} + \lambda_3(t_1 P_{b,1} + \mu^{-1} P_{b,2} - E)$ , where  $\lambda_i$  with  $i \in \{1, 2, 3\}$  are Lagrange multipliers, the Karush–Kuhn–Tucker (KKT) conditions can be expressed as follows:

$$\frac{\mu t_1 2^{-\frac{N_a}{t_1}} \tilde{h}_b}{\ln 2 \left( 1 + \left( 1 - 2^{-\frac{N_a}{t_1}} \right) \tau + 2^{-\frac{N_a}{t_1}} \rho_{b,1} |h_b|^2 \right)} + \lambda_3 t_1 - \lambda_1 = 0, \tag{A1a}$$

$$\frac{\tilde{h}_b}{\ln 2 (1 + \rho_{b,2} |h_b|^2)} + \lambda_3 \mu^{-1} - \lambda_2 = 0, \tag{A1b}$$

$$t_1 P_{b,1} + \mu^{-1} P_{b,2} - E \leq 0, \tag{A1c}$$

$$\lambda_3 (t_1 P_{b,1} + \mu P_{b,2} - E) = 0, \tag{A1d}$$

$$-P_{b,i} \leq 0, \forall i \in \{1, 2\}, \tag{A1e}$$

$$\lambda_i P_{b,i} = 0, \forall i \in \{1, 2\}, \tag{A1f}$$

$$\lambda_i \geq 0, \forall i \in \{1, 2, 3\}. \tag{A1g}$$

For the hybrid RSMA-TDMA case, since  $\lambda_i = 0, \forall i \in \{1, 2\}$ , and hence  $P_{b,1}$  and  $P_{b,2}$  are non-zero, which is the reason this case is termed hybrid RSMA. If  $\lambda_3 = 0$ , the KKT conditions are as follows:

$$\frac{\mu t_1 B 2^{-\frac{N_a}{t_1 B}} \frac{\ell_b |h_b|^2}{\sigma^2}}{\ln 2(1+(1-2^{-\frac{L_a}{t_1}})\tau+2^{-\frac{L_a}{t_1}} \rho_{b,1} |h_b|^2)} = 0, \quad (\text{A2a})$$

$$\frac{\frac{\ell_b |h_b|^2}{\sigma^2}}{\ln 2(1+\rho_{b,2} |h_b|^2)} = 0, \quad (\text{A2b})$$

which cannot be true. Therefore, we can show that  $\lambda_3 \neq 0$  as follows, which means that the KKT conditions can be rewritten as:

$$\frac{\mu t_1 B 2^{-\frac{N_a}{t_1 B}} \frac{\ell_b |h_b|^2}{\sigma^2}}{\ln 2(1+(1-2^{-\frac{N_a}{t_1 B}})\tau+2^{-\frac{N_a}{t_1 B}} \rho_{b,1} |h_b|^2)} + \lambda_3 t_1 = 0, \quad (\text{A3a})$$

$$\frac{B \frac{\ell_b |h_b|^2}{\sigma^2}}{\ln 2(1+\rho_{b,2} |h_b|^2)} + \lambda_3 \mu^{-1} = 0, \quad (\text{A3b})$$

$$t_1 P_{b,1} + \mu^{-1} P_{b,2} - E = 0, \quad (\text{A3c})$$

$$P_{b,i} > 0, \forall i \in \{1, 2\}. \quad (\text{A3d})$$

With some algebraic operations, the optimal solutions of  $P_{b,1}$  and  $P_{b,2}$  can be obtained as shown in Lemma 1.

## References

- Iwai, T.; Nakao, A. Demystifying Myths of MEC: Rethinking and Exploring Benefits of Multi-Access/Mobile Edge Computing. In Proceedings of the 2018 IEEE 7th International Conference on Cloud Networking (CloudNet), Tokyo, Japan, 22–24 October 2018; pp. 1–4.
- Wang, H.; Lv, T.; Lin, Z.; Zeng, J. Energy-Delay Minimization of Task Migration Based on Game Theory in MEC-Assisted Vehicular Networks. *IEEE Trans. Veh. Technol.* **2022**, *71*, 8175–8188. [\[CrossRef\]](#)
- Shirin Abkenar, F.; Ramezani, P.; Iranmanesh, S.; Murali, S.; Chulerttiyawong, D.; Wan, X.; Jamalipour, A.; Raad, R. A Survey on Mobility of Edge Computing Networks in IoT: State-of-the-Art, Architectures, and Challenges. *IEEE Commun. Surv. Tuts.* **2022**, *24*, 2329–2365. [\[CrossRef\]](#)
- Shirin Abkenar, F.; Iranmanesh, S.; Bouguettaya, A.; Raad, R.; Jamalipour, A. ENERAGENT: An energy-efficient UAV-assisted fog-IoT framework for disaster management. *J. Commun. Netw.* **2022**, *24*, 698–709. [\[CrossRef\]](#)
- Altin, I.; Akar, M. Novel OMA and Hybrid NOMA Schemes for MEC Offloading. In Proceedings of the 2020 IEEE International Black Sea Conference on Communications and Networking (BlackSeaCom), Odessa, Ukraine, 26–29 May 2020; pp. 1–5.
- Kiani, A.; Ansari, N. Edge Computing Aware NOMA for 5G Networks. *IEEE Internet Thing J.* **2018**, *5*, 1299–1306. [\[CrossRef\]](#)
- Wan, Z.; Xu, D.; Xu, D.; Ahmad, I. Joint computation offloading and resource allocation for NOMA-based multi-access mobile edge computing systems. *Comput. Netw.* **2021**, *196*, 108256. [\[CrossRef\]](#)
- Chen, G.; Wu, Q.; Chen, W.; Ng, D.W.K.; Hanzo, L. IRS-Aided Wireless Powered MEC Systems: TDMA or NOMA for Computation Offloading? *IEEE Trans. Wirel. Commun.* **2023**, *22*, 1201–1218. [\[CrossRef\]](#)
- Ding, Z.; Ng, D.W.K.; Schober, R.; Poor, H.V. Delay Minimization for NOMA-MEC Offloading. *IEEE Signal Process. Lett.* **2018**, *25*, 1875–1879. [\[CrossRef\]](#)
- Liu, L.; Sun, B.; Wu, Y.; Tsang, D.H.K. Latency Optimization for Computation Offloading with Hybrid NOMA-OMA Transmission. *IEEE Internet Thing J.* **2021**, *8*, 6677–6691. [\[CrossRef\]](#)
- Zeng, M.; Nguyen, N.P.; Dobre, O.A.; Poor, H.V. Delay Minimization for NOMA-Assisted MEC Under Power and Energy Constraints. *IEEE Wirel. Commun. Lett.* **2019**, *8*, 1657–1661. [\[CrossRef\]](#)
- Zhou, F.; You, C.; Zhang, R. Delay-Optimal Scheduling for IRS-Aided Mobile Edge Computing. *IEEE Wirel. Commun. Lett.* **2021**, *10*, 740–744. [\[CrossRef\]](#)
- Li, H.; Fang, F.; Ding, Z. Joint resource allocation for hybrid NOMA-assisted MEC in 6G networks. *Digit. Commun. Netw.* **2020**, *6*, 241–252. [\[CrossRef\]](#)
- Mao, Y.; Dizdar, O.; Clerckx, B.; Schober, R.; Popovski, P.; Poor, H.V. Rate-Splitting Multiple Access: Fundamentals, Survey, and Future Research Trends. *IEEE Commun. Surv. Tuts.* **2022**, *24*, 2073–2126. [\[CrossRef\]](#)
- Xu, Y.; Mao, Y.; Dizdar, O.; Clerckx, B. Rate-Splitting Multiple Access With Finite Blocklength for Short-Packet and Low-Latency Downlink Communications. *IEEE Trans. Veh. Technol.* **2022**, *71*, 12333–12337. [\[CrossRef\]](#)

16. Xiao, F.; Li, X.; Yang, L.; Liu, H.; Tsiftsis, T.A. Outage Performance Analysis of RSMA-Aided Semi-Grant-Free Transmission Systems. *IEEE Open J. Commun. Soc.* **2023**, *4*, 253–268. [[CrossRef](#)]
17. Rimoldi, B.; Urbanke, R. A rate-splitting approach to the Gaussian multiple-access channel. *IEEE Trans. Inf. Theory* **1996**, *42*, 364–375. [[CrossRef](#)]
18. Mao, Y.; Clerckx, B.; Li, V.O.K. Rate-splitting multiple access for downlink communication systems: bridging, generalizing, and outperforming SDMA and NOMA. *EURASIP J. Wirel. Commun. Netw.* **2018**, *2018*, 133. [[CrossRef](#)] [[PubMed](#)]
19. Clerckx, B.; Mao, Y.; Jorswieck, E.A.; Yuan, J.; Love, D.J.; Erkip, E.; Niyato, D. A Primer on Rate-Splitting Multiple Access: Tutorial, Myths, and Frequently Asked Questions. *IEEE J. Select. Areas Commun.* **2023**, *41*, 1265–1308. [[CrossRef](#)]
20. Clerckx, B.; Mao, Y.; Schober, R.; Poor, H.V. Rate-Splitting Unifying SDMA, OMA, NOMA, and Multicasting in MISO Broadcast Channel: A Simple Two-User Rate Analysis. *IEEE Wirel. Commun. Lett.* **2020**, *9*, 349–353. [[CrossRef](#)]
21. Jaafar, W.; Naser, S.; Muhaidat, S.; Sofotasios, P.C.; Yanikomeroglu, H. On the Downlink Performance of RSMA-Based UAV Communications. *IEEE Trans. Veh. Technol.* **2020**, *69*, 16258–16263. [[CrossRef](#)]
22. Ye, Z.; Wang, X.; Zhang, Z.; Chen, X.; Yan, C. A rate-splitting non-orthogonal multiple access scheme for uplink transmission. In Proceedings of the International Conference on Wireless Communications & Signal Processing, Chennai, India, 22–24 March 2017.
23. Liu, H.; Tsiftsis, T.A.; Kim, K.J.; Kwak, K.S.; Poor, H.V. Rate Splitting for Uplink NOMA with Enhanced Fairness and Outage Performance. *IEEE Trans. Wirel. Commun.* **2020**, *19*, 4657–4670. [[CrossRef](#)]
24. Yang, Z.; Chen, M.; Saad, W.; Xu, W.; Shikh-Bahaei, M. Sum-Rate Maximization of Uplink Rate Splitting Multiple Access (RSMA) Communication. *IEEE Trans. Mob. Comput.* **2022**, *21*, 2596–2609.
25. Truong, T.P.; Dao, N.N.; Cho, S. HAMEC-RSMA: Enhanced Aerial Computing Systems with Rate Splitting Multiple Access. *IEEE Access* **2022**, *10*, 52398–52409. [[CrossRef](#)]
26. Liu, H.; Bai, Z.; Lei, H.; Pan, G.; Kim, K.J.; Tsiftsis, T.A. A New Rate Splitting Strategy for Uplink CR-NOMA Systems. *IEEE Trans. Veh. Technol.* **2022**, *71*, 7947–7951. [[CrossRef](#)]
27. Liu, H.; Ye, Y.; Bai, Z.; Kim, K.J.; Tsiftsis, T.A. Rate Splitting Multiple Access Aided Mobile Edge Computing in Cognitive Radio Networks. In Proceedings of the 2022 IEEE International Conference on Communications Workshops (ICC Workshops), Seoul, Republic of Korea, 16–20 May 2022; pp. 598–603.
28. Chen, P.; Liu, H.; Ye, Y.; Yang, L.; Kim, K.J.; Tsiftsis, T.A. Rate-Splitting Multiple Access Aided Mobile Edge Computing With Randomly Deployed Users. *IEEE J. Select. Areas Commun.* **2023**, *41*, 1549–1565. [[CrossRef](#)]
29. Wang, F.; Xu, J.; Ding, Z. Optimized Multiuser Computation Offloading with Multi-Antenna NOMA. In Proceedings of the 2017 IEEE Globecom Workshops (GC Wkshps), Singapore, 4–8 December 2017; pp. 1–7.
30. Sabuj, S.R.; Asiedu, D.K.P.; Lee, K.J.; Jo, H.S. Delay Optimization in Mobile Edge Computing: Cognitive UAV-Assisted eMBB and mMTC Services. *IEEE Trans. Cogn. Commun. Netw.* **2022**, *8*, 1019–1033. [[CrossRef](#)]
31. Dinkelbach, W. On Nonlinear Fractional Programming. *Manag. Sci.* **1967**, *13*, 492–498. [[CrossRef](#)]

**Disclaimer/Publisher’s Note:** The statements, opinions and data contained in all publications are solely those of the individual author(s) and contributor(s) and not of MDPI and/or the editor(s). MDPI and/or the editor(s) disclaim responsibility for any injury to people or property resulting from any ideas, methods, instructions or products referred to in the content.